

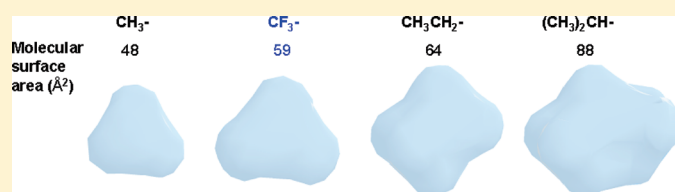
Influence of Fluorocarbon and Hydrocarbon Acyl Groups at the Surface of Bovine Carbonic Anhydrase II on the Kinetics of Denaturation by Sodium Dodecyl Sulfate

Andrew Lee, Katherine A. Mirica, and George M. Whitesides*

Department of Chemistry and Chemical Biology, Harvard University 12 Oxford St., Cambridge, Massachusetts 02138, United States

Supporting Information

ABSTRACT: This paper examines the influence of acylation of the Lys- ϵ -NH $_3^+$ groups of bovine carbonic anhydrase (BCA, EC 4.2.1.1) to Lys- ϵ -NHCOR (R = $-\text{CH}_3$, $-\text{CH}_2\text{CH}_3$, and $-\text{CH}(\text{CH}_3)_2$, $-\text{CF}_3$) on the rate of denaturation of this protein in buffer containing sodium dodecyl sulfate (SDS). Analysis of the rates suggested separate effects due to electrostatic charge and hydrophobic interactions. Rates of denaturation ($k_{\text{Ac},n}$) of each series of acylated derivatives depended on the number of acylations (n). Plots of $\log k_{\text{Ac},n}$ vs n followed U-shaped curves. Within each series of derivatives, rates of denaturation decreased as n increased to ~ 7 ; this decrease was compatible with increasingly unfavorable electrostatic interactions between SDS and protein. In this range of n , rates of denaturation also depended on the choice of the acyl group as n increased to ~ 7 , in a manner compatible with favorable hydrophobic interactions between SDS and the $-\text{NHCOR}$ groups. As n increased in the range $7 < n < 14$, however, rates of denaturation stayed approximately constant; analysis suggested that these rates were compatible with an increasingly important contribution to denaturation that depended both on the net negative charge of the protein and on the hydrophobicity of the R group. The mechanism of denaturation thus seems to change with the extent of acylation of the protein. For derivatives with the same net electrostatic charge, rates of denaturation increased with the acyl group (by a factor of ~ 3 for $n \sim 14$) in the order $\text{CH}_3\text{CONH}- < \text{CH}_3\text{CH}_2\text{CONH}- < (\text{CH}_3)_2\text{CHCONH}- < \text{CF}_3\text{CONH}-$. These results suggested that the hydrophobicity of $\text{CF}_3\text{CONH}-$ is slightly greater (by a factor of < 2) than that of $\text{RHCONH}-$ with similar surface area.



INTRODUCTION

This paper describes the rates of denaturation of bovine carbonic anhydrase II (BCA, EC 4.2.1.1) derivatized with fluorocarbon acyl groups ($\text{CF}_3\text{CONH}-$) and hydrocarbon acyl groups of similar surface area [$\text{R}_\text{H}\text{CONH}-$; $\text{R}_\text{H} = \text{CH}_3-$, CH_3CH_2- , or $(\text{CH}_3)_2\text{CH}-$] in solutions containing sodium dodecyl sulfate (SDS). By comparing rates, we address two problems: (i) the mechanism of denaturation of these proteins in SDS and (ii) whether the hydrophobicity of fluorocarbons is distinguishable from that of hydrocarbons in protein chemistry.

Our measure of the influence of $\text{CF}_3\text{CONH}-$ and $\text{R}_\text{H}\text{CONH}-$ groups on the properties (especially stability) of BCA was the rate of denaturation of $\text{BCA}-[\text{CF}_3\text{CONH}-]_n$ and $\text{BCA}-[\text{R}_\text{H}\text{CONH}-]_n$ in solutions of SDS (3.0 mM in Tris–Gly buffer: 25 mM Tris–192 mM glycine, pH = 8.4, 22 °C). Analysis of reaction mixtures of protein and SDS by capillary electrophoresis (CE) allowed us to measure rates of denaturation conveniently and simultaneously for all acylated proteins having the same R. This ability to measure the same reaction occurring with large numbers of different proteins at the same time was essential in building sets of comparable data for different R. We interpreted the kinetics of denaturation in terms of increases in the hydrophobicity of the surface of the protein upon acylation and concomitant decreases in the number of charged groups (and corresponding increases in the net negative charge of the protein). Although the mechanism for the denaturation of BCA by SDS is still not completely

understood,^{1–5} the kinetics suggested a dependence on the hydrophobic interactions of the acyl groups, with SDS and with neighboring groups at the surface of BCA, and a contribution from the net charge of the protein.

For $\text{BCA}-[\text{CF}_3\text{CONH}-]_n$ and $\text{BCA}-[\text{R}_\text{H}\text{CONH}-]_n$, rates of denaturation ($\log k_{\text{Ac},n}$) followed a U-shaped curve with n . Rates decreased with n in the range 0–7 (by factors of ~ 10 –30), remained approximately constant with n in the range 7–14, and increased as n increased beyond ~ 15 . A difference between the rates of denaturation for $\text{BCA}-[\text{CF}_3\text{CONH}-]_n$ and $\text{BCA}-[\text{R}_\text{H}\text{CONH}-]_n$ emerged and increased as n increased to ~ 7 . $\text{BCA}-[\text{CF}_3\text{CONH}-]_n$ denatured more rapidly than $\text{BCA}-[\text{R}_\text{H}\text{CONH}-]_n$ with the same electrostatic charge (by factors of ~ 2 –3 when $n = 14$). The rates of denaturation suggested that the hydrophobicity of $\text{CF}_3\text{CONH}-$ groups is greater than that of $\text{R}_\text{H}\text{CONH}-$ groups and is not determined by surface area alone. According to this method of inferring the “hydrophobicity” of groups at the surface of a protein—primary amides generated by the acylation of Lys- ϵ -NH $_3^+$ groups— CF_3- groups are slightly more hydrophobic than $\text{R}_\text{H}-$ (per unit surface area). The hydrophobicity of $\text{CF}_3\text{CONH}-$ is still less than that of $\text{CH}_3(\text{CH}_2)_4\text{CONH}-$ (based on the analysis of

Received: August 16, 2010

Revised: December 5, 2010

Published: December 23, 2010

BCA-[CH₃(CH₂)₄CONH-]_n in a previously reported study.¹ The hydrophobicity of CF₃CONH- and R_HCONH- groups analyzed and distinguished in this study includes contributions from both the hydrophobicity of CF₃- and R_H- groups and the effect of these groups on the noncovalent interactions of the adjacent -CONH- group.

In the range $7 \leq n \leq 14$, BCA-[CF₃CONH-]_n denatured more rapidly than BCA-[R_HCONH-]_n, but the difference in rates of denaturation of BCA-[CF₃CONH-]_n and of BCA-[R_HCONH-]_n was approximately constant for each R group. This observation suggested rates of denaturation that are independent of the number of acylations but still depend upon whether the protein is derivatized with CF₃CONH- or R_HCONH- groups. We addressed this apparent contradiction by analytical modeling of the curves for $\log k_{Ac,n}$. The kinetics of denaturation suggests a change in the mechanism as the number of acylations increased beyond ~ 7 to one in which both the net negative charge of the protein and the hydrophobicity of the R group contribute to destabilization. Despite the complexity in the mechanisms of denaturation of BCA, these rates of denaturation suggest that CF₃CONH- groups are slightly but distinguishably more hydrophobic than R_HCONH- with similar surface area; this difference is a composite of the intrinsic hydrophobicity of R_H- and CF₃- groups and the influence of these groups (we assume through inductive effects) on the polarity of the directly bonded amide groups.

Physical Properties of Fluorocarbon Groups. Incorporation of F- or CF₃- is an important tool in the design of ligands for proteins.^{6–10} The contact angle of water is greater on surfaces presenting CF₃- groups than that on surfaces presenting CH₃- groups (118° and 112°, on self-assembled monolayers of CF₃- or CH₃-terminated alkanethiolates on gold);¹¹ the broad impression is that fluorocarbons are “more hydrophobic” than hydrocarbons.^{12–14} Are they more hydrophobic, and is any difference evident in the context of molecular recognition in biochemistry? Fluorine substitution has been exploited to influence the solubility, acid–base properties, and binding affinity of ligands;^{8,12} in addition, fluorine substitution can increase the bioavailability and metabolic stability of pharmaceuticals.⁷ In the design of proteins, the use of fluorocarbon groups has been aimed at stabilizing tertiary and quaternary structure, directing protein–protein interactions, and modifying protein–lipid interactions.^{15–20} Previous studies have examined the effect of non-native amino acids (e.g., hexafluoroleucine, trifluorovaline) on the stability of small proteins and on the assembly of helical peptides into oligomeric structures, in which CF₃- groups are positioned within the hydrophobic core.^{16,17,21–26} Substitution of fluorocarbons for structurally analogous hydrocarbons, in most cases, increases the resistance of these structures to thermal and chemical denaturation. Although CF₃- groups appear to be more hydrophobic than CH₃- groups, it is unclear whether surface area (which is larger for CF₃- than for CH₃-) or some other property determines the hydrophobicity of fluorocarbon groups. Fluorocarbon groups are less polarizable (per unit of molecular volume) than their hydrocarbon analogs^{13,27} and are also distinguished from hydrocarbons by the polarity and inductive effect of C–F bonds.^{12,13} An understanding of how these properties influence molecular recognition, particularly at the surfaces of proteins, remains incomplete.

One objective of this paper was to compare the influence of CF₃CONH- and hydrocarbon acyl groups of similar surface area on the properties of a well-understood model protein. Our underlying question was whether the hydrophobic interactions

Table 1. Comparison of Properties of Fluorocarbons and Hydrocarbons

property	H	F	ref
atomic radius (Å)	1.20	1.47	12
covalent bond length, C–X (Å)	1.09	1.38	12
molecular surface area (Å ²)			
CX ₃ –H	46	59	33
CH ₃ CH ₂ –H	64		
(CH ₃) ₂ CH–H	80		
(CH ₃) ₂ (CH ₂) ₅ –H	132		
$\pi_R = \log(P_{R-C_6H_5}/P_{C_6H_5})$			
CX ₃ –	0.56	0.88	12
C ₂ X ₅ –	1.02		
CX ₃ O–	–0.02	1.04	
CX ₃ S–	0.61	1.44	
CX ₃ CO–	0.02	0.55	
CX ₃ CONH–	–1.27	0.08	
CX ₃ SO ₂ –	–1.63	0.55	
$\pi_R = \log(P_{R-CONHCH_2-C_6H_5}/P_{C_6H_5})$ ³⁴			
CX ₃ –	–0.2	0.95	34
CH ₃ CH ₂ –	0.07		
(CH ₃) ₂ CH–	0.35		
CH ₃ (CH ₂) ₃ CH ₂ –	1.52		
dipole moment, μ (D)			
CF ₃ –X	1.65	0	12
CF ₃ –CX ₃	2.32	0	
pK _a			
CX ₃ CO ₂ H	4.8	0.5	12
CX ₃ CH ₂ NH ₃ ⁺	10.7	5.9	
CX ₃ SO ₂ NH ₂	10.5	5.8	
CX ₃ CH ₂ OH	15.9	12.4	
n_D^{20}			
n-C ₅ X ₁₂	1.3573	1.2383	12
γ (dyn/cm)			
n-C ₈ X ₁₈	21.8	13.6	12
δ (cal/cm ³) ^{1/2}			
n-C ₇ X ₁₆	7.4	6.0	35

of CF₃CONH- and R_HCONH- groups are determined only by the surface area of these groups or whether fluorocarbon groups are more hydrophobic (by some appropriate metric) than hydrocarbon groups of similar surface area. We addressed this question indirectly by analyzing the interactions of sodium dodecyl sulfate (SDS) with derivatives of BCA modified with CF₃CONH- or R_HCONH- groups, generated by the acylation of Lys- ϵ -NH₃⁺ (BCA-[CF₃CONH-]_n with $n \leq 15$; BCA-[R_HCONH-]_n with $n \leq 17$ –18).

Hydrophobicity, Evaluated by Partitioning in Water–Octanol (Table 1). Are fluorocarbons more hydrophobic than hydrocarbons with similar surface area? Hansch parameters (π) describe substituent effects on the partitioning of R–C₆H₅ in water–octanol mixtures.²⁸ Values of π for R–C₆H₅ indicate that the hydrophobicity of CF₃– ($\pi = 0.88$) lies between that of CH₃– ($\pi = 0.56$) and CH₃CH₂– ($\pi = 1.02$) and suggest a correlation between the hydrophobicity and the solvent-exposed surface areas of these groups.²⁹

Values of π also, however, depend on hydrogen-bonding^{30,31} and potentially include contributions from the inductive effect of CF₃–, through the polarization of groups that accept or

donate hydrogen bonds. As a result, differences in π between compounds with CF_3 — groups and those with CH_3 — groups depend on the neighboring group and range from 0.3 to 2.2 for the examples in Table 1.^{12,32} Among the data in Table 1, values of π for $\text{R}-\text{CONH}-\text{CH}_2\text{C}_6\text{H}_5$ are the most relevant for comparing the hydrophobicity of acyl groups evaluated in this study. Values of π show that $\text{CF}_3\text{CONH}-$ groups are more hydrophobic than $(\text{CH}_3)_2\text{CHCONH}-$, although they have a lower surface area. This example emphasizes the importance of the neighboring $-\text{CONH}-$ group. This order of hydrophobicity might reflect an intrinsic difference between fluoroalkyl and alkyl groups of the same area. The inductive effect of CF_3- might, however, also contribute to the hydrophobicity of $\text{CF}_3\text{CONH}-$, by weakening the ability of $-\text{C}(\text{O})-$ to accept hydrogen bonds from water (to a greater extent than increasing the ability of $\text{N}-\text{H}$ to donate hydrogen bonds to water).^{36,37}

Further discussion of the comparison of the properties in Table 1 is available in the Supporting Information.

■ EXPERIMENTAL DESIGN

Protein Charge Ladders: Variation of Electrostatic Charge and Surface Hydrophobicity. Charge ladders of a protein are families of derivatives of that protein, obtained by sequential acylation of $\text{Lys-}\epsilon\text{-NH}_3^+$ groups; the derivatives differ in the number of modifications at the surface and in net electrostatic charge.^{1,38} Since acylation of $\text{Lys-}\epsilon\text{-NH}_3^+$ simultaneously eliminates a positively charged group and adds an acyl group to the surface of proteins, this chemical modification has the potential to perturb both the electrostatic and hydrophobic interactions of derivatized proteins.

Unacylated BCBA in the native state has a net negative electrostatic charge of ~ 3.3 units in the buffer solutions we used (25 mM Tris–192 mM glycine, pH = 8.4).³⁹ Acylation of $\text{Lys-}\epsilon\text{-NH}_3^+$ groups increases the amount of net negative charge of the protein by ~ 0.9 units (the amount is less than a full unit due to charge regulation).^{38,40} $\text{BCA}-[\text{CH}_3\text{CONH}-]_{18}$ therefore has ~ 19 units of net negative charge.^{41–43} A derivative of BCA with the greatest number of $\text{CF}_3\text{CONH}-$ that we could prepare, $\text{BCA}-[\text{CF}_3\text{CONH}-]_{15}$, has a net negative charge of ~ 17 units.

Each of the 18 lysine residues of BCA is located at the surface of BCA and is exposed to solvent. We believe that the acylation of surface-exposed $\text{Lys-}\epsilon\text{-NH}_3^+$ groups is largely random, although specific $\text{Lys-}\epsilon\text{-NH}_3^+$ groups may be especially reactive or unreactive.⁴⁴ “Rungs” of charge ladders are mixtures of regioisomers that have the same number of acylations but differ from each other in the sites of acylated Lys residues, distributed over the surface of the protein.³⁸ The use of charge ladders to analyze the effect of acylation on the properties of a protein relies on the behavior of mixtures of regioisomers to reveal the average effect of acylation, taken over all sites of acylated Lys.¹ This approach requires the approximation that the properties of derivatized proteins depend on n and the type of acyl group (e.g., $\text{CF}_3\text{CONH}-$ or $\text{R}_\text{H}\text{CONH}-$) but do not depend on which Lys residues are acylated; we do not consider interactions of the acyl groups that may be specific to the site of acylation.

We wished to evaluate the contribution of hydrophobic interactions due to $\text{CF}_3\text{CONH}-$ groups on the surface of a protein in a way that was independent of the influence of acylation on electrostatic interactions. Our strategy was to compare the properties of corresponding rungs of the charge ladders $\text{BCA}-[\text{CF}_3\text{CONH}-]_n$ and $\text{BCA}-[\text{R}_\text{H}\text{CONH}-]_n$. We assumed that the increase in net negative charge caused by the acylation of $\text{Lys-}\epsilon\text{-NH}_3^+$ groups

was the same for the formation of $\text{CF}_3\text{CONH}-$ and $\text{R}_\text{H}\text{CONH}-$ groups and that both types of acylation were random. We assumed that by comparing $\text{BCA}-[\text{CF}_3\text{CONH}-]_n$ and $\text{BCA}-[\text{R}_\text{H}\text{CONH}-]_n$ having the same charge, we would be able to attribute differences in the properties of these proteins to the hydrophobic interactions of $\text{CF}_3\text{CONH}-$ and $\text{R}_\text{H}\text{CONH}-$ at the surface of BCA, rather than to electrostatic interactions reflecting the conversion of $-\text{NH}_3^+$ to $\text{RCONH}-$ groups.

The first-order effects of acylation are the elimination of positive charge and the increase in hydrophobic surface area. Acylation of $\text{Lys-}\epsilon\text{-NH}_3^+$ also generates an amide. The properties of $\text{BCA}-[\text{CF}_3\text{CONH}-]_n$ and $\text{BCA}-[\text{R}_\text{H}\text{CONH}-]_n$ potentially include contributions from the hydrogen bonds of the amides generated by acylation. We expected the inductive effect of CF_3- groups to influence the hydrogen bonding of $-\text{CONH}-$ groups, by weakening the hydrogen bonds involving $-\text{C}(\text{O})-$ and by strengthening hydrogen bonds donated by $\text{N}-\text{H}$;⁴⁵ we could not, however, predict how it would ultimately affect the properties of derivatives of BCA.^{46–48} Details concerning hydrogen bonds at the surface of BCA or its acylated derivatives, in aqueous solution, are not known (i.e., whether $-\text{CONH}-$ groups are hydrogen-bonded to water molecules or to neighboring groups at the surface of BCA).⁴⁹

Selection of $\text{R}_\text{H}\text{CONH}-$ Groups. We chose to analyze charge ladders of BCA with $\text{CH}_3\text{CONH}-$, $\text{CH}_3\text{CH}_2\text{CONH}-$, $(\text{CH}_3)_2\text{CHCONH}-$ groups for two reasons: (i) these groups have surface areas that are similar to that of the $\text{CF}_3\text{CONH}-$ group (Table 1) and (ii) we anticipated the preparation of approximately complete charge ladders of BCA with these groups (with n up to 15) to be straightforward since preparation of $\text{BCA}-[\text{CH}_3\text{CONH}-]_{18}$ is straightforward.⁴³

Previous Study of the Denaturation of Charge Ladders of BCA by SDS. Rates of Denaturation Depend on the Electrostatic Charge and Surface Hydrophobicity of BCA. Gudiksen et al. compared charge ladders of BCA with acetyl and hexanoyl groups ($\text{BCA}-[\text{CH}_3\text{CONH}-]_n$ and $\text{BCA}-[\text{CH}_3(\text{CH}_2)_4\text{CONH}-]_n$) to probe the electrostatic and hydrophobic interactions involved in the denaturation of BCA by SDS.¹ For both charge ladders, rates of denaturation in 3.0 mM SDS followed a U-shaped curve with the number of acylations, n (Figure 1A). The curves drawn in Figure 1 were obtained by the fit of $\Delta G_n^\ddagger = a + bn + cn^2$ to the data. ΔG_n^\ddagger is the free energy of activation; values for ΔG^\ddagger were determined from the rate constants, k , with the equation $k = A \exp(-\Delta G^\ddagger/2.3RT)$ (A is the prefactor in transition state theory; a value of $\sim 10^6 \text{ s}^{-1}$ was used for A , an empirical estimate calculated for the folding of a small protein, cytochrome *c*).⁵⁰

In Gudiksen's study, the values of the coefficient b quantified the difference in the hydrophobic interactions of hexanoyl groups and acetyl groups; the values for a characterized ΔG^\ddagger for unacylated BCA, and the values for c suggested electrostatic interactions that did not depend on the choice of the acyl group. For a variety of reasons that emerge upon examination of a broader range of acyl groups (see Results and Discussion), we now infer that $\text{CH}_3\text{CONH}-$ and $\text{CH}_3(\text{CH}_2)_4\text{CONH}-$ are both atypical and use an analysis of the data based on $k = k_1(n) + k_2(n)$, where k_1 and k_2 are the rate constants for competing mechanisms of denaturation.

Electrostatic Interactions. The study by Gudiksen proposed two types of electrostatic interactions that contribute to the denaturation of BCA: (i) intermolecular electrostatic repulsion between SDS and BCA, responsible for the decrease in rates for n in the range 0–8, and (ii) intramolecular repulsion between negatively charged groups on BCA, responsible for the destabilization of folded BCA and increase the rates for $n > 9$ (for hexanoyl) or $n > 12$ (for acetyl).

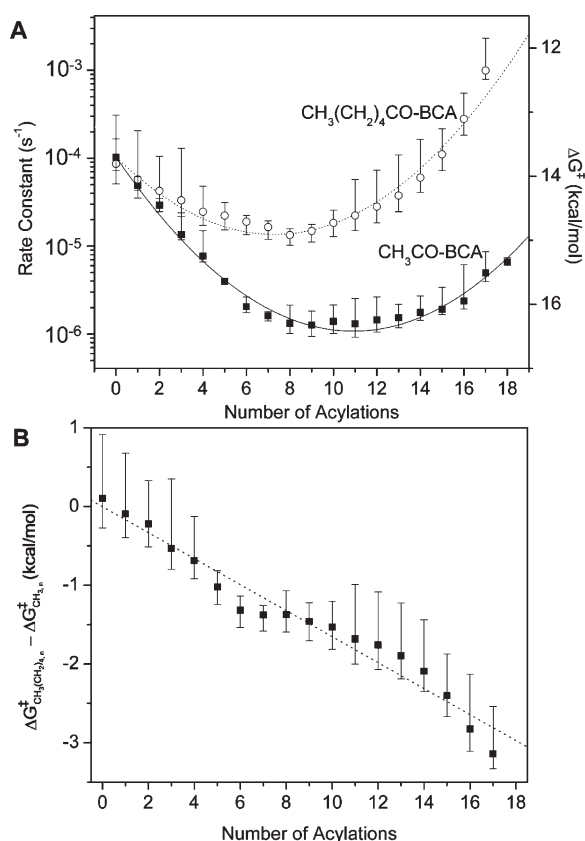


Figure 1. (A) Pseudo-first-order rate constants of denaturation for $\text{BCA}-[\text{CH}_3\text{CONH-}]_n$ and $\text{BCA}-[\text{CH}_3(\text{CH}_2)_4\text{CONH-}]_n$ previously reported by Gudiksen et al.¹ Charge ladders were denatured in solutions of 3.0 mM SDS in 25 mM Tris–192 mM Gly, pH = 8.4. Kinetics were determined by analyzing the decrease in folded protein in each rung, using the same experimental procedures used in this paper. Curves were obtained by fitting points to the equation $\Delta G_n^\ddagger = a + bn + cn^2$; ref 1 derives a model to justify the equation and interpret the curves. (B) Differences in ΔG_n^\ddagger between derivatives with $\text{CH}_3\text{CONH-}$ and $\text{CH}_3(\text{CH}_2)_4\text{CONH-}$ groups for each rung. A line with slope $0.17 \text{ kcal mol}^{-1}$ per group fits the points ($r^2 = 0.97$). Reproduced with permission from ref 1. Copyright 2006 Biophysical Society, American Physical Society.

Measuring the Contribution of Hydrophobic Interactions. Denaturation was more rapid for $\text{BCA}-[\text{CH}_3(\text{CH}_2)_4\text{CONH-}]_n$ than for $\text{BCA}-[\text{CH}_3\text{CONH-}]_n$ and suggested a contribution from hydrophobic interactions over the entire range of n (0–17). The quantity $\Delta G_{\text{CH}_3(\text{CH}_2)_4\text{CO-BCA}}^\ddagger - \Delta G_{\text{CH}_3\text{CO-BCA}}^\ddagger$, plotted in Figure 1B, is the difference in the free energy of activation for derivatives with the same electrostatic charge; the values measure the difference in the hydrophobic interactions between hexanoyl and acetyl groups involved in the rate-limiting step of denaturation. In this analysis, the dependence of $\Delta G_{\text{CH}_3(\text{CH}_2)_4\text{CO-BCA}}^\ddagger - \Delta G_{\text{CH}_3\text{CO-BCA}}^\ddagger$ on n was approximately linear and suggested that adding hydrophobic groups to the surface of BCA decreased the kinetic stability of BCA by $\sim 0.20 \text{ kcal mol}^{-1} \text{ nm}^{-2}$. While the mechanism of denaturation of BCA by SDS remains unknown, these results suggested that the acyl groups at the surface of derivatives of BCA contribute to the rate-determining step of denaturation, through hydrophobic interactions with SDS and with nearby groups at the surface of BCA.

Capillary Electrophoresis. We analyzed charge ladders of BCA by resolving them on the basis of electrophoretic mobility, $\mu_{\text{Ac},n}$. In eq 1, $\mu_{\text{Ac},n}$ is expressed as a function of the electrostatic

charge of native BCA (Z_0 ; ~ -3.3 in Tris–Gly buffer, pH = 8.4),³⁹ the molecular weight of BCA (M_{BCA}), the number of acylations (n), the change in electrostatic charge caused by the acylation of each Lys- $\epsilon\text{-NH}_3^+$ group (ΔZ ; ~ 0.9),^{38,40} and the molecular weight of the acyl group (M_{Ac}). The shape of the protein and other factors that relate the molecular weight to a hydrodynamic radius determine the value of α (often approximated as $2/3$ for globular proteins); C_p is a constant.

$$\mu_{\text{Ac},n} = C_p \frac{Z_0 + n\Delta Z}{(M_{\text{BCA}} + nM_{\text{Ac}})^\alpha} \quad (1)$$

Peaks in CE represent derivatives having the same net electrostatic charge (“rungs”) and allow us to know the number of acylations. Rungs observed in CE are mixtures of regioisomers having the same number of surface modifications. We expected, and found, values of $\mu_{\text{Ac},n}$ to be insensitive to the type of acyl group because M_{Ac} is less than 0.3% of M_{BCA} and $\Delta Z \sim -0.9$ for each acyl group used in this paper.³⁸

CE is able to resolve folded protein in charge ladders (4–18 $\text{cm}^2 \text{ kV}^{-1} \text{ min}^{-1}$) from complexes of denatured protein and SDS ($\sim 21 \text{ cm}^2 \text{ kV}^{-1} \text{ min}^{-1}$; μ is approximately the same for all derivatives in the denatured state). Absorbance at 214 nm detects BCA in both its folded and denatured forms and is insensitive to SDS, which is transparent at 214 nm.

Procedure for Analyzing the Kinetics of Denaturation of $\text{BCA}-[\text{CF}_3\text{CONH-}]_n$ and $\text{BCA}-[\text{R}_\text{H}\text{CONH-}]_n$. Tris–Gly Buffer with 3.0 mM SDS. We denatured $\text{BCA}-[\text{CF}_3\text{CONH-}]_n$ and $\text{BCA}-[\text{R}_\text{H}\text{CONH-}]_n$ in solutions of 3.0 mM SDS in Tris–Gly buffer (25 mM Tris–192 mM glycine, pH = 8.4).⁵¹ We chose the concentration 3.0 mM for two reasons: (i) denaturation in 3.0 mM SDS was slow (reactions take place over ~ 2 –50 h) and allowed us to measure the kinetics of denaturation by analyzing reaction mixtures by CE (20 min per run) and (ii) a concentration of SDS below the critical micellar concentration (cmc) avoided complications involving micelles (the cmc is ~ 4.0 mM in Tris–Gly buffer).¹

Addition of SDS by Dialysis. In order to maintain an approximately constant concentration of 3.0 mM for free SDS (i.e., SDS that is not associated to protein) over the course of the reaction, we dialyzed samples of protein against solutions of SDS.^{1,52} This procedure resulted in the denaturation of $\text{BCA}-[\text{CF}_3\text{CONH-}]_n$ and $\text{BCA}-[\text{CH}_3\text{CONH-}]_n$ with pseudo-first-order kinetics. By analyzing the decrease in the areas of peaks for folded $\text{BCA}-[\text{CF}_3\text{CONH-}]_n$ and $\text{BCA}-[\text{R}_\text{H}\text{CONH-}]_n$ in CE data, we determined pseudo-first-order rate constants for denaturation ($k_{\text{Ac},n}$).

Analysis of the Denaturation of Charge Ladders in Parallel. Each experiment consisted of analyzing the denaturation of two charge ladders—that of $\text{BCA}-[\text{CF}_3\text{CONH-}]_n$ and $\text{BCA}-[\text{R}_\text{H}\text{CONH-}]_n$ —in parallel. Analysis of samples in parallel was essential for distinguishing the rates of denaturation of $\text{BCA}-[\text{CF}_3\text{CONH-}]_n$ and $\text{BCA}-[\text{R}_\text{H}\text{CONH-}]_n$. Since rates of denaturation are sensitive to the concentration of SDS (the rate of denaturation of BCA increases by $\sim 10^4$ in the range of 2.5–4.0 mM SDS),⁴³ the experimental error in preparing reservoirs of 3.0 mM SDS contributed to the uncertainty in the rates. This source of experimental uncertainty was eliminated by comparing the rates of denaturation of $\text{BCA}-[\text{CF}_3\text{CONH-}]_n$ and $\text{BCA}-[\text{R}_\text{H}\text{CONH-}]_n$ measured by denaturing both samples in the same reservoir of SDS and analyzing them in parallel.

RESULTS AND DISCUSSION

Synthesis of Charge Ladders of BCA. Derivatization of BCA with $\text{CF}_3\text{CONH-}$ Groups. We surveyed several $\text{CF}_3\text{CO-L}$ (where L

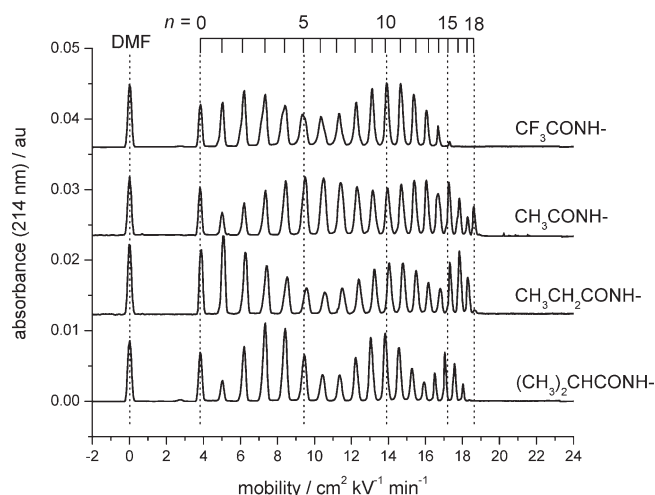
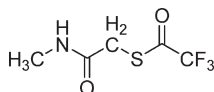


Figure 2. Charge ladders of BCA with $\text{CF}_3\text{CONH}-$ and $\text{R}_\text{H}\text{CONH}-$ groups. Charge ladders were obtained by combining several reaction mixtures that varied in the extent of acylation of BCA; proteins were purified from hydrolysis products and reaction buffer by gel filtration chromatography. Samples for CE consisted of charge ladders (100 μM in BCA over all rungs) in Tris–Gly buffer (25 mM Tris–192 mM glycine, pH = 8.4); N,N -dimethylformamide (DMF; 1 mM) was added to serve as a neutral marker for electro-osmotic flow. Analysis by CE (30 kV) used bare, fused-silica capillaries (107 cm in length, 100 μm between inlet and detector) and Tris–Gly running buffer.

is a leaving group) for the generation of $\text{BCA}-[\text{CF}_3\text{CONH}-]_n$ in aqueous buffer (see Supporting Information for details). Acylation of $\text{Lys-}\epsilon\text{-NH}_3^+$ groups with S -(2-mercapto- N -methylacetamide)thio-trifluoroacetate (**1**) in solutions of 0.2 M sodium borate (pH = 10.0) produced the best results: charge ladders containing derivatives having up to 15 $\text{CF}_3\text{CONH}-$ groups.



1

We used **1**, in amounts corresponding to 40–250 equiv per lysine residue, to prepare several mixtures of $\text{BCA}-[\text{CF}_3\text{CONH}-]_n$. Combining these mixtures, each consisting of a distribution in n , resulted in a nearly complete charge ladder of $\text{BCA}-[\text{CF}_3\text{CONH}-]_n$. Analysis by CE resolved the charge ladder into rungs on the basis of $\mu_{\text{Ac},n}$ (top trace in Figure 2).

Efforts to generate derivatives with more than 15 $\text{CF}_3\text{CONH}-$ groups, and ultimately peracylated derivatives, were unsuccessful. The yield of reactions with **1** (and other $\text{CF}_3\text{CO}-\text{L}$ with BCA) was poor compared to that of reactions with other acetylating agents; $\text{BCA}-[\text{CH}_3\text{CONH}-]_{18}$, for example, can be prepared in ~90% yield by reaction of BCA with 20 equiv of acetic anhydride. The solubility of **1** (20–50 mg/mL) and the buffer capacity of the solution limited the concentrations of **1** we could use. Reactions of $\text{BCA}-[\text{CF}_3\text{CONH}-]_n$ with a second batch of **1** in fresh buffer resulted in mixtures of proteins that could not be resolved by CE (broad peak at $\sim 13 \text{ cm}^2 \text{ kV}^{-1} \text{ min}^{-1}$) and were probably substantially denatured (CE data available in the Supporting Information). These proteins did not associate with dansyl amide (DNSA), an arylsulfonamide inhibitor of BCA; analysis by size-exclusion chromatography showed a retention time corresponding to a molecular weight greater than that of

monomeric BCA. These observations suggested that derivatization with more than 15 $\text{CF}_3\text{CONH}-$ groups results in denaturation, and probably aggregation, of BCA.

Derivatization of BCA with $\text{R}_\text{H}\text{CONH}-$ Groups. Reactions of BCA with the N -hydroxysuccinimide esters of acetate, propanoate, and 2-methyl-2-propanoate in buffered solutions (pH = 9.0, 0.1 M HEPBS) generated mixtures of $\text{BCA}-[\text{CH}_3\text{CONH}-]_n$, $\text{BCA}-[\text{CH}_3\text{CH}_2\text{CONH}-]_n$, and $\text{BCA}-[(\text{CH}_3)_2\text{CHCONH}-]_n$, respectively. Analysis of charge ladders by CE showed derivatives having up to 17–18 acylations (Figure 2). Variation in quantities across rungs in ladders has no significance and is solely an artifact of preparing ladders by mixing several batches of $\text{BCA}-[\text{R}_\text{H}\text{CONH}-]_n$. A complete charge ladder for $\text{BCA}-[\text{CH}_3\text{CONH}-]_n$ was prepared by adding $\text{BCA}-[\text{CH}_3\text{CONH}-]_{18}$ (prepared separately) to a charge ladder with $n = 0$ –17.⁴² Charge ladders for $\text{BCA}-[\text{CH}_3\text{CH}_2\text{CONH}-]_n$ and $\text{BCA}-[(\text{CH}_3)_2\text{CHCONH}-]_n$ contained derivatives with $n = 0$ –17; we did not attempt to prepare samples of BCA peracylated in these groups.

Derivatives of BCA with $\text{CF}_3\text{CONH}-$ or $\text{R}_\text{H}\text{CONH}-$ groups were folded and monomeric.⁵³ Proteins comprising the charge ladders bound DNSA with the same stoichiometry as native BCA (determined by fluorescence of DNSA in solutions containing 0.2 μM BCA).⁴² We inferred that $\text{BCA}-[\text{CF}_3\text{CONH}-]_n$ and $\text{BCA}-[\text{R}_\text{H}\text{CONH}-]_n$ bind Zn^{2+} in the active site and have the same tertiary structure as unmodified BCA, since both properties are required for binding arylsulfonamide inhibitors.⁵⁴

Denaturation of $\text{BCA}-[\text{CF}_3\text{CONH}-]_n$ and $\text{BCA}-[\text{R}_\text{H}\text{CONH}-]_n$ in 3.0 mM SDS. *Analysis of Mixtures by CE.* We analyzed the denaturation of $\text{BCA}-[\text{CF}_3\text{CONH}-]_n$ and $\text{BCA}-[\text{R}_\text{H}\text{CONH}-]_n$ in parallel. In each experiment, we loaded two samples— $\text{BCA}-[\text{CF}_3\text{CONH}-]_n$ and either $\text{BCA}-[\text{CH}_3\text{CONH}-]_n$, $\text{BCA}-[\text{CH}_3\text{CH}_2\text{CONH}-]_n$, or $\text{BCA}-[(\text{CH}_3)_2\text{CHCONH}-]_n$ —into dialysis cassettes (10 kDa molecular weight cutoff). Denaturation by SDS was initiated by placing the samples (1.0 mL, 60 μM in protein) into reservoirs of 3.0 mM SDS in Tris–Gly buffer (2.0 L, 22 °C). We monitored the denaturation of charge ladders by removing aliquots (100 μL s) from the dialysis cassettes and analyzing them by CE, at time points up to 30–150 h. Samples were analyzed by CE using running buffer (Tris–Gly) containing 3.0 mM SDS. Injections in CE experiments consumed $\sim 10 \text{ nL}$ s of sample; aliquots were returned to the dialysis cassette after sampling and were out of the reservoir of 3.0 mM SDS for less than 5 min. Figure 3 shows a set of electropherograms taken from a representative run analyzing the denaturation of $\text{BCA}-[\text{CF}_3\text{CONH}-]_n$ and $\text{BCA}-[(\text{CH}_3)_2\text{CHCONH}-]_n$, chosen from four repetitions of the experiment. Data for the analysis of $\text{BCA}-[\text{CH}_3\text{CONH}-]_n$ and $\text{BCA}-[\text{CH}_3\text{CH}_2\text{CONH}-]_n$ are available in the Supporting Information.

Folded derivatives of BCA separated into rungs (4 – $18 \text{ cm}^2 \text{ kV}^{-1} \text{ min}^{-1}$) in CE; complexes of denatured protein with SDS appeared as a single, broad peak at higher mobility ($\sim 21 \text{ cm}^2 \text{ kV}^{-1} \text{ min}^{-1}$), reflecting an increase in negative charge caused by the association of a large number of equivalents of SDS.^{5,55} The number of equivalents of SDS is probably close to ~ 150 , based on the broadly observed stoichiometry of 1.4 g of SDS per 1 g of protein for complexes prepared for analysis by SDS–PAGE (polyacrylamide gel electrophoresis).⁵ All derivatives of BCA denatured in 3.0 mM SDS, over periods of time spanning ~ 2 –100 h.

Measurement of the Rates of Denaturation. The decrease in the areas of peaks for folded protein allowed us to measure the rates of denaturation for $\text{BCA}-[\text{CF}_3\text{CONH}-]_n$ and $\text{BCA}-[\text{R}_\text{H}\text{CONH}-]_n$. The Supporting Information contains a discussion of the quantitative treatment of electropherograms, including procedures

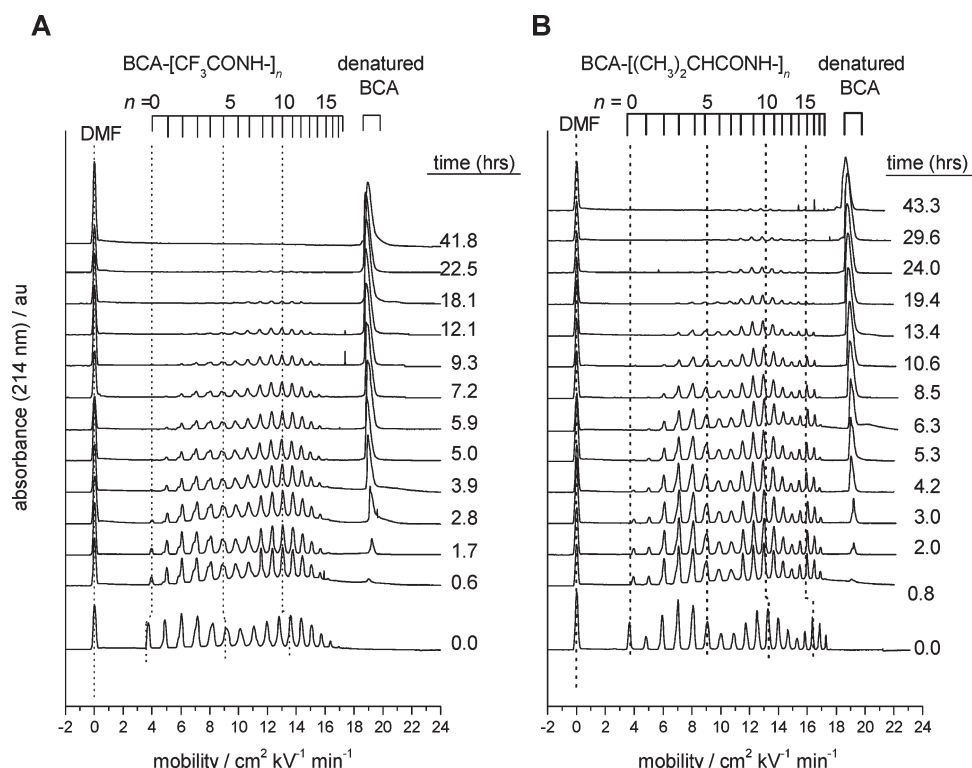


Figure 3. Denaturation of $\text{BCA}-[\text{CF}_3\text{CONH}-]_n$ and $\text{BCA}-[(\text{CH}_3)_2\text{CHCONH}-]_n$ in 3.0 mM SDS. Aliquots from reaction mixtures were analyzed by CE (30 kV) using capillaries (107 cm in length, 100 cm between inlet and detector) filled with Tris–Gly buffer and 3.0 mM SDS. To serve as an internal standard and report on the electro-osmotic flow, DMF (1 mM) was added to the aliquots prior to injection. Absorbance at 214 nm detected derivatives of BCA in the folded state and in complexes with SDS. Prior to the addition of SDS, charge ladders were analyzed by CE in running buffer without SDS (electropherograms at the bottom of each set, labeled with “0.0 h”). Mobilities were slightly higher in buffer without SDS than in buffer with 3.0 mM SDS. The shift to lower values of mobility in solutions of SDS was consistent with screening of the charge of proteins by SDS; addition of 3.0 mM SDS increased the ionic strength of the buffer from ~ 8.3 to ~ 11.3 mM.

to account for differences in the amount of time spent at the UV-detector and decreases in the concentration of protein in reaction mixtures over time ($<10\%$ over 72 h).⁵⁶ Figure 4 shows the analysis of the decrease in folded $\text{BCA}-[\text{CF}_3\text{CONH}-]_n$ and $\text{BCA}-[(\text{CH}_3)_2\text{CHCONH}-]_n$ over time. The points represent the amount of folded protein in each rung, expressed as a fraction of the amount of folded protein before the addition of SDS. Lines were obtained by fitting a single-exponential decay to the points. Of the three $\text{BCA}-[\text{R}_\text{H}\text{CONH}-]_n$ tested, $\text{BCA}-[(\text{CH}_3)_2\text{CHCONH}-]_n$ denatured at rates that were closest to those of $\text{BCA}-[\text{CF}_3\text{CONH}-]_n$. Data for the denaturation of the other charge ladders are available in the Supporting Information.

Although the denaturation of 60 μM BCA corresponds to the binding of an amount of SDS that exceeds the amount of SDS in a reaction mixture of 3.0 mM SDS, the addition of SDS to the reaction mixture by dialysis maintained an approximately constant concentration of SDS (3.0 mM). This protocol, and the reasonable fit of a single-exponential decay to the points ($r^2 > 0.9$ for the fit to data covering ~ 3 half-lives), allowed us to interpret the data using pseudo-first-order kinetics and to estimate the rate constants of denaturation for each rung, $k_{\text{AC},n}$.

Kinetics of Denaturation of $\text{BCA}-[\text{CF}_3\text{CONH}-]_n$ and $\text{BCA}-[\text{R}_\text{H}\text{CONH}-]_n$. The plots in Figure 5 show the rate constants of denaturation ($k_{\text{AC},n}$) for $\text{BCA}-[\text{CF}_3\text{CONH}-]_n$ and $\text{BCA}-[\text{R}_\text{H}\text{CONH}-]_n$. For each charge ladder, the rate constants traced U-shaped curves similar to those observed in the analysis of $\text{BCA}-[\text{CH}_3\text{CONH}-]_n$ and $\text{BCA}-[\text{CH}_3(\text{CH}_2)_4\text{CONH}-]_n$ by Gudiksen et al.¹ Within a series of acylated derivatives of BCA, rate constants

varied by factors of 10–30 as n increased to ~ 15 . These data confirmed that the modification of BCA, by acylation of $\text{Lys-}\epsilon\text{-NH}_3^+$ groups, caused systematic variation in the rates of denaturation of acylated derivatives of BCA by SDS. Acylation simultaneously increased the net electrostatic charge and the hydrophobicity of the surface of BCA; the dependence of $k_{\text{AC},n}$ on n thus characterized the perturbation of both electrostatic and hydrophobic interactions involved in the interaction of BCA with SDS. We developed a model to interpret the shape of the curves for $k_{\text{AC},n}$ in terms of these interactions (discussed briefly in a later section). The mathematical model and fitting procedure are provided in detail in the Supporting Information; we were primarily interested in using the data for $k_{\text{AC},n}$ in Figure 5 to distinguish the hydrophobicity of $\text{CF}_3\text{CONH}-$ and $\text{R}_\text{H}\text{CONH}-$ groups.

Distinguishing the Hydrophobicity of $\text{CF}_3\text{CONH}-$ and $\text{R}_\text{H}\text{CONH}-$. To evaluate the difference in hydrophobicity between $\text{CF}_3\text{CONH}-$ and $\text{R}_\text{H}\text{CONH}-$ groups at the surface of BCA, we compared the rates of denaturation of derivatives with the same number of acylations. The quantity $\Delta G_{\text{R}_\text{H}}^\ddagger - \Delta G_{\text{CF}_3}^\ddagger$, calculated using the rate constants of denaturation $k_{\text{CF}_3,n}$ and $k_{\text{R}_\text{H},n}$, is the difference in the free energy of activation for the denaturation of $\text{BCA}-[\text{R}_\text{H}\text{CONH}-]_n$ and $\text{BCA}-[\text{CF}_3\text{CONH}-]_n$ (eq 2).

$$\Delta G_{\text{R}_\text{H}}^\ddagger - \Delta G_{\text{CF}_3}^\ddagger = 2.3RT \log \left(\frac{k_{\text{CF}_3,n}}{k_{\text{R}_\text{H},n}} \right) \quad (2)$$

Since $\Delta G_{\text{R}_\text{H}}^\ddagger - \Delta G_{\text{CF}_3}^\ddagger$ describes the difference in rate between proteins with the same net electrostatic charge, values of

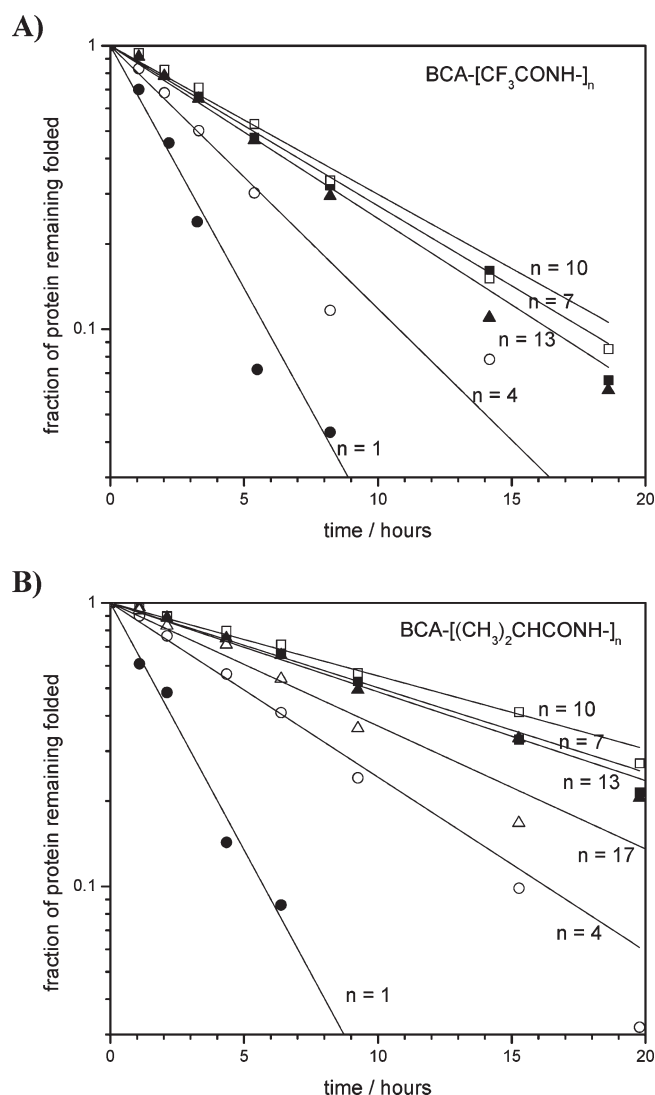


Figure 4. Rates of denaturation determined by the decrease in areas of peaks for folded protein. Points show the amount of folded protein in runs for (A) $\text{BCA}-[\text{CF}_3\text{CONH-}]_n$ and (B) $\text{BCA}-[(\text{CH}_3)_2\text{CHCONH-}]_n$, determined from areas of peaks observed in CE; the amount of folded protein is expressed as a fraction of the initial amount of folded protein (i.e., prior to the addition of SDS). Plots show data for $n = 1, 4, 7, 10$, and 13 for visual clarity. Data are from one of four repetitions of the experiment; we do not show experimental uncertainties because the times at which reaction mixtures were analyzed varied across repetitions. Lines fitting the points represent single-exponential decay and were obtained by fitting the equation $2.3RT \log(A_t A_0^{-1}) = -kt$, where A_t and A_0 are the areas of peaks at times t and 0 h after the addition of SDS, and k is the pseudo-first-order rate constant (R is the Boltzmann constant and T is the temperature).

$\Delta G_{\text{R}_\text{H}}^\mp - \Delta G_{\text{CF}_3}^\mp$ are useful for comparing the hydrophobic interactions of $\text{BCA}-[\text{CF}_3\text{CONH-}]_n$ and $\text{BCA}-[\text{R}_\text{H}\text{CONH-}]_n$ in a way that is independent of the influence of acylation on electrostatic interactions. Figure 6 shows values of $\Delta G_{\text{R}_\text{H}}^\mp - \Delta G_{\text{CF}_3}^\mp$ determined from the rates of denaturation of $\text{BCA}-[\text{CF}_3\text{CONH-}]_n$ and $\text{BCA}-[\text{R}_\text{H}\text{CONH-}]_n$ measured for samples analyzed in parallel (for $\text{R}_\text{H} = \text{CH}_3-$, CH_3CH_2- , or $(\text{CH}_3)_2\text{CH}-$). For the comparison of $\text{BCA}-[\text{CF}_3\text{CONH-}]_n$ with $\text{BCA}-[(\text{CH}_3)_2\text{CHCONH-}]_n$, we calculated $\Delta G_{\text{R}_\text{H}}^\mp - \Delta G_{\text{CF}_3}^\mp$ using data from separate sets of experiments, by adding $\Delta G_{\text{CH}_3(\text{CH}_2)_4}^\mp - \Delta G_{\text{CH}_3}^\mp$ (taken from the analysis in ref 1) to $\Delta G_{\text{CH}_3}^\mp - \Delta G_{\text{CF}_3}^\mp$ (determined from

experiments for this paper); error bars are larger than those in the other sets of data because they include propagation of error over the two sets of experiments.

$\text{BCA}-[\text{CF}_3\text{CONH-}]_n$ denatured more rapidly than each of the $\text{BCA}-[\text{R}_\text{H}\text{CONH-}]_n$ analyzed in this study ($\text{R}_\text{H} = \text{CH}_3-$, CH_3CH_2- , or $(\text{CH}_3)_2\text{CH}-$). Values of $\Delta G_{\text{R}_\text{H}}^\mp - \Delta G_{\text{CF}_3}^\mp$ reached 0.4 – 0.6 kcal mol⁻¹ for derivatives with $n \sim 14$, corresponding to rates of denaturation that were greater for derivatives with $\text{CF}_3\text{CONH-}$ groups than those for derivatives with $\text{R}_\text{H}\text{CONH-}$ groups, by factors of 2 – 3 . The increase in $\Delta G_{\text{R}_\text{H}}^\mp - \Delta G_{\text{CF}_3}^\mp$ with n at low levels of acylation ($n \leq 7$) described the increasing influence of hydrophobic interactions on the rate of denaturation, as the surface of BCA was made increasingly hydrophobic by sequential acylation. For derivatives with $n > 7$, however, further changes in $\Delta G_{\text{R}_\text{H}}^\mp - \Delta G_{\text{CF}_3}^\mp$ with increasing n were small; values of $\Delta G_{\text{R}_\text{H}}^\mp - \Delta G_{\text{CF}_3}^\mp$ were approximately constant for $n > 7$ in the comparison of $\text{BCA}-[\text{CF}_3\text{CONH-}]_n$ with $\text{BCA}-[\text{CH}_3\text{CH}_2\text{CONH-}]_n$ or $\text{BCA}-[(\text{CH}_3)_2\text{CHCONH-}]_n$. The fit of lines to data in separate ranges of n distinguished the trends in $\Delta G_{\text{R}_\text{H}}^\mp - \Delta G_{\text{CF}_3}^\mp$ at “low” ($0 \leq n \leq 7$) and “moderate” ($7 \leq n \leq 14$) numbers of acylations; the slopes of the lines decreased by factors > 5 (dotted lines in Figure 6).

We drew two conclusions from the results in Figure 6: (i) $\text{CF}_3\text{CONH-}$ groups are “more hydrophobic” (by 0.05 – 0.07 kcal mol⁻¹ per group) than $\text{R}_\text{H}\text{CONH-}$ groups with the same surface area (i.e., $\text{R}_\text{H} = \text{CH}_3\text{CH}_2-$ or $(\text{CH}_3)_2\text{CH}-$). The hydrophobicity of $\text{CF}_3\text{CONH-}$ groups is not determined by molecular surface area alone and is thus distinguished from that of $\text{R}_\text{H}\text{CONH-}$ groups by some other property of CF_3- groups. (We discuss the possibility that the inductive effect of CF_3- on the hydrogen-bonding of $-\text{CONH-}$ contributes to hydrophobicity in a later section). The difference in hydrophobicity between $\text{CF}_3\text{CONH-}$ and $\text{R}_\text{H}\text{CONH-}$ groups is not large; however, $\text{CF}_3\text{CONH-}$ groups are still less hydrophobic than $\text{CH}_3(\text{CH}_2)_4\text{CONH-}$ groups. (ii) The factors that determine the rates of denaturation change as the number of acylations increases beyond $n \sim 7$. For $n = 7$ – 14 , there is little change in the rate of denaturation for $\text{CF}_3\text{CONH-}$ and all of the $\text{R}_\text{H}\text{CONH-}$ groups ($\text{CH}_3(\text{CH}_2)_4\text{CONH-}$ is less well-behaved than the others) as $\text{R}_\text{H}\text{CONH-}$ groups are added.

Interpretation of Rates in Terms of Hydrophobicities of the Acyl Groups. The interpretation of the kinetic data in Figures 5 and 6 suggests that there are three kinetic regimes. Identifying and characterizing these regimes is straightforward, although full interpretation of them is complicated. Fortunately, in order to interpret these data in terms of the relative hydrophobicity of the acylating groups used, a full mechanistic interpretation is not necessary.

i. Denaturation Slowed by Acylation: Repulsion of SDS ($n = 0$ – 8).

In this region, increasing the extent of acylation decreases the rate of denaturation. The data are compatible with the hypothesis that this regime is dominated by the net charge on the protein (or by the number of NH_3^+ groups), but that the trends with n describing these changes are slightly modified by the hydrophobicity of the acyl groups. A plausible mechanistic interpretation is that acylation of $\text{Lys-}\epsilon\text{-NH}_3^+$ decreases the equilibrium association of an equivalent of SDS but that increasingly hydrophobic R_H groups result in a smaller decrease in association. Thus, acylation (making the protein more negatively charged or eliminating positive charges; the data cannot distinguish) decreases the association of SDS with the protein; increasing the hydrophobicity of the acyl groups makes the association of SDS less unfavorable (or, relative to other rungs of the charge ladder, more

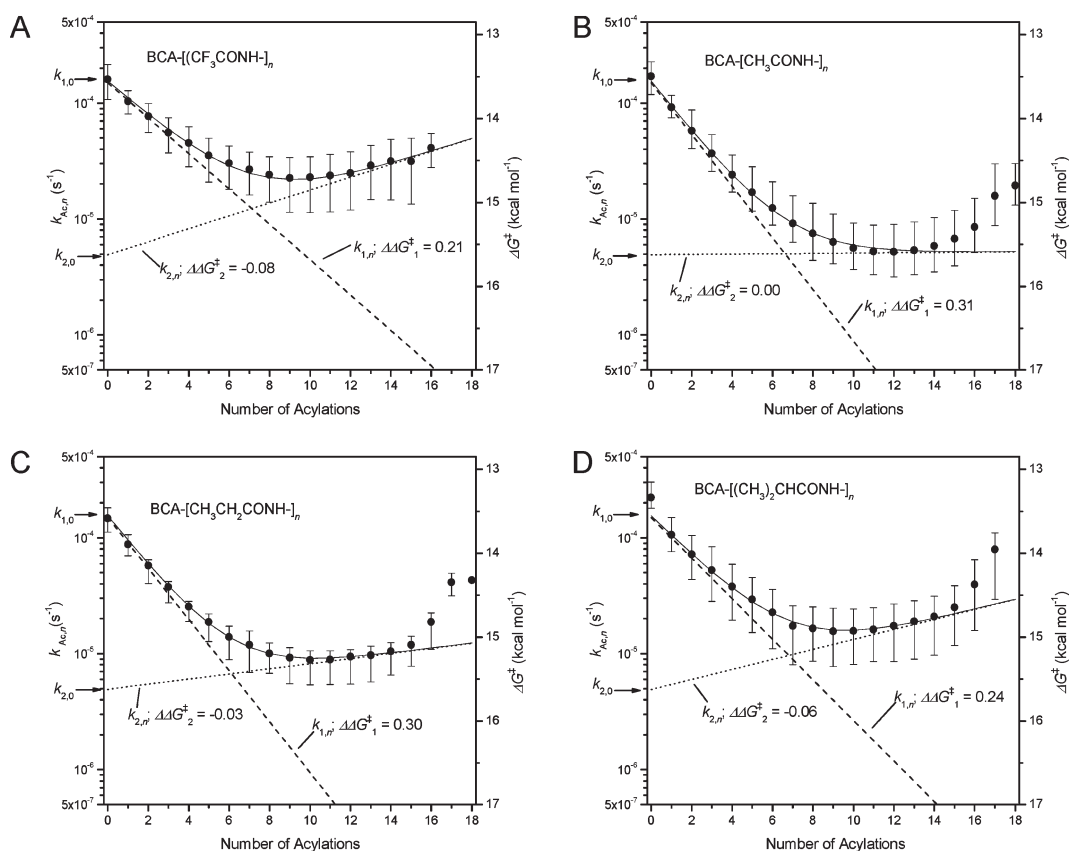


Figure 5. Kinetics of Denaturation of $\text{BCA}-[\text{CF}_3\text{CONH}-]_n$ and $\text{BCA}-[\text{R}_H\text{CONH}-]_n$. In each plot, points are average values of the pseudo-first-order rate constant, $k_{\text{Ac},n}$. In part A, error bars represent the standard deviation for $k_{\text{CF}_3,n}$ measured in 12 repetitions. In parts B–D, the error bars span minimum and maximum values of $k_{\text{R}_H,n}$ measured in four repetitions. Solid curved lines were obtained by the fit of eq S1 (Supporting Information) to the points, with the adjustable parameters $k_{1,0}$, $k_{2,0}$, $\Delta\Delta G_1^\ddagger$, $\Delta\Delta G_2^\ddagger$. Fits were generally good in the range of $0 \leq n \leq 14$. The curves consist of contributions from $k_{1,n}$ (dashed line) and $k_{2,n}$ (dotted line). Values of $\Delta\Delta G_1^\ddagger$, $\Delta\Delta G_2^\ddagger$ are in units of kcal mol^{-1} per group; slopes of the lines for $\log k_{1,n}$ and $\log k_{2,n}$ represent the quantities $-\Delta\Delta G_1^\ddagger/2.3RT$ and $-\Delta\Delta G_2^\ddagger/2.3RT$, and are unitless. The y-axis to the right of the plots is a scale for the free energy of activation (ΔG^\ddagger) and was approximated by the same method used in Figure 1.

favorable). The influence of hydrophobicity of the $\text{RCONH}-$ group (relative to the case $R = \text{CF}_3$) increases in the order (cal mol^{-1} per group) $R = \text{CH}_3-$ ($\Delta\Delta G_H = 65$), CH_3CH_2- ($\Delta\Delta G_H = 57$), $(\text{CH}_3)_2\text{CH}-$ ($\Delta\Delta G_H = 54$), CF_3- ($\Delta\Delta G_H = 0$), and $\text{CH}_3-(\text{CH}_2)_4-$ ($\Delta\Delta G_H = -132$). (Note that these numbers are in calories, not kilocalories!) Thus, by this ranking, CF_3 lies in between $(\text{CH}_3)_2\text{CH}$ and $\text{CH}_3(\text{CH}_2)_4$, although closer to the former. We analyze this order in more detail below.

ii. *Denaturation Independent of Electrostatics; Very Weakly Dependent on Hydrophobicity ($n = 9-14$).* In this regime, Figures 4 and 5 suggest that the mechanism of unfolding changes to one in which the extent of acetylation is relatively unimportant (although there is a similar trend with hydrophobicity), where contributions from relative hydrophobicity are a factor of ~ 10 smaller than in regime 1.

iii. *Denaturation Strongly Promoted by Acylation ($n > 14$).* In this regime, acylation accelerates unfolding and suggests that a separate process takes over denaturation. Data for derivatives with $\text{R}_H\text{CONH}-$ groups show this trend clearly; data for $\text{BCA}-[\text{CF}_3\text{CONH}-]_n$ in this regime are incomplete. These data are compatible with the hypothesis that electrostatic repulsions between groups on derivatives of BCA with large amounts of net negative charge (>17 units) destabilize the native structure of BCA. In this regime, these intramolecular interactions may be more important to the kinetics of

denaturation than the association of BCA and SDS. We have not analyzed this regime further; the available data do not allow us to draw conclusions about contributions from the hydrophobicity of the acyl groups.

The Relative Hydrophobicity of $\text{CF}_3\text{CONH}-$ Groups Cannot Be Explained by Molecular Surface Area Alone. The rates of denaturation of $\text{BCA}-[\text{CF}_3\text{CONH}-]_n$ and $\text{BCA}-[\text{R}_H\text{CONH}-]_n$ suggest that the hydrophobicity of $\text{CF}_3\text{CONH}-$ is greater than that expected on the basis of surface area alone: that is, the fluorocarbon is slightly more hydrophobic than the corresponding hydrocarbon of the same solvent-accessible surface area.

To support the hypothesis that $\text{BCA}-[\text{CF}_3\text{CONH}-]_n$ denatures more rapidly than $\text{BCA}-[\text{R}_H\text{CONH}-]_n$ as a result of the hydrophobic interactions of $\text{CF}_3\text{CONH}-$ and $\text{R}_H\text{CONH}-$ groups at the surface of BCA, we measured the effect of $\text{CF}_3\text{CONH}-$ and $\text{R}_H\text{CONH}-$ groups on the water–octanol partitioning of a model compound. We chose to analyze the partitioning of $\text{CF}_3\text{CONH}-\text{CH}_2\text{C}_6\text{H}_5$ and $\text{R}_H\text{CONH}-\text{CH}_2\text{C}_6\text{H}_5$ for three reasons: (i) These compounds contain the same functional group (primary amide) used to modify BCA and are thus good models for $\text{CF}_3\text{CONH}-$ and $\text{R}_H\text{CONH}-$ of acylated Lys residues at the surface of BCA. Water–octanol partitioning of these compounds should also include potential contributions from the inductive effect of CF_3- and R_H- on hydrogen bonds involving $-\text{CONH}-$ groups. (ii) These

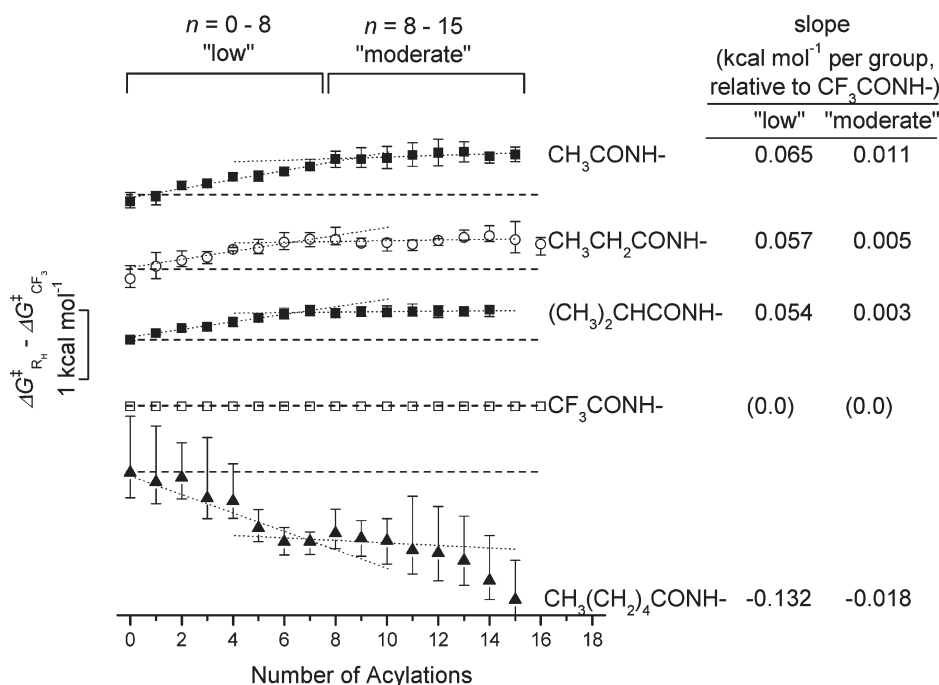


Figure 6. Difference in the rates of denaturation of derivatives of BCA with the same electrostatic charge. Values of $\Delta G_{R_n}^{\ddagger} - \Delta G_{CF_3n}^{\ddagger}$ were determined from k_{CF_3n} and k_{R_n} measured in parallel in each repetition of the denaturation of $BCA-[CF_3CONH-]_n$ and $BCA-[R_nCONH-]_n$ in parallel. Each set of data is shown with a floating y-axis; the dashed lines represent a value of $0.0 \text{ kcal mol}^{-1}$. Points are average values, and error bars reach minimum and maximum values found in four repetitions. Dotted lines were obtained by least-squares fit to the data in selected ranges. Lines for "low" numbers of acylation used data with $0 \leq n \leq 8$ ($R_H = CH_3-$) or $0 \leq n \leq 7$ ($R_H = CH_3CH_2-$ or $(CH_3)_2CH-$), while lines for "moderate" levels of acylation used data with $8 \leq n \leq 14$ ($R_H = CH_3-$) or $7 \leq n \leq 14$ ($R_H = CH_3CH_2-$ or $(CH_3)_2CH-$). Values of $\Delta G_{R_n}^{\ddagger} - \Delta G_{CF_3n}^{\ddagger}$ were not obtained for $n > 15$ because $BCA-[CF_3CONH-]_n$ with $n > 15$ could not be prepared. Values of slope for CF_3CONH- are (0.0) by the definition of $\Delta G_{R_n}^{\ddagger} - \Delta G_{CF_3n}^{\ddagger}$.

compounds are easy to synthesize. (iii) Analysis of the water–octanol partitioning of these compounds is convenient. Values of π measured for $CF_3CONH-CH_2C_6H_5$ and $R_nCONH-CH_2C_6H_5$ are in Table 1 (experimental procedures for the synthesis of compounds and analysis of water–octanol partitioning are in the Supporting Information).

Figure 7A shows values of $\Delta\Delta G_1^{\ddagger}$ and $\Delta\Delta G_2^{\ddagger}$ (slopes of the lines for $\log k_{1,n}$ and $\log k_{2,n}$ in Figure 5, multiplied by the factor $-2.3RT$) plotted against values of π . This plot correlates the measurements of the hydrophobicity of CF_3CONH- and R_nCONH- from two methods: (i) analysis of the rates of denaturation of BCA (a model protein), derivatized at the surface by these groups, in solutions of SDS and (ii) analysis of the influence of these groups on water–octanol partitioning. The plot shows qualitative agreement between these methods—the order in hydrophobicity is the same for $\Delta\Delta G_1^{\ddagger}$, $\Delta\Delta G_2^{\ddagger}$, and π —and supports the conclusion that CF_3CONH- groups at the surface of BCA are more hydrophobic than hydrocarbon acyl groups with similar surface area. Water–octanol partitioning provides only a crude model for the interactions of CF_3CONH- and R_nCONH- groups in the denaturation of BCA; as a result, we do not draw quantitative conclusions from this correlation.

The plot in Figure 7B shows the relationship between molecular surface area and π for CF_3CONH- and R_nCONH- groups. The points for the hydrocarbon acyl groups (R_nCONH- and $CH_3-(CH_2)_4CONH-$) show a good correlation of surface area with hydrophobicity. The partitioning of $CF_3CONH-CH_2C_6H_5$ shows that CF_3CONH- groups are more hydrophobic (by ~ 1 log unit) than hydrocarbon acyl groups of similar surface area. The underlying reason for the hydrophobicity of CF_3CONH- groups is not clear

and not entirely resolved by these data; it may involve both the low polarizability of the CF_3- group and the influence of CF_3- on the properties of the adjacent amide group.

CONCLUSIONS

"Hydrophobicity" is Defined Only Qualitatively by These Experiments. The system that we describe has strengths and weaknesses. Its three strengths: (i) It examines the concept of hydrophobicity (or, perhaps, more exactly, "effective hydrophobicity of the $RCONH-$ group") in the context of a process that involves protein, in a typical aqueous buffer; it thus measures "hydrophobicity" empirically (defined in our experiments as the propensity to promote the association of SDS to a model protein) but in a way relevant to the influence of perfluorocarbons on molecular recognition in biology. (ii) It generates large numbers of directly comparable data taken from parallel analysis of many rungs of protein charge ladders and thus gives meaningful quantitative estimates for small effects. (iii) By comparing charge ladders, it separates electrostatic and hydrophobic contributions to the denaturation of BCA and derivatives in SDS. It also has three weaknesses. (i) the denaturation of BCA in SDS is clearly a very complicated process, which is apparently different for members of a charge ladder as the number of acylations increases. The mechanisms for denaturation are suggested by these data, but important details remain unproven. (ii) It is plausible, but unproven, that the effects attributed to hydrophobicity of the acyl groups are caused by the association of the hydrocarbon chains of SDS with the surface of the protein. (iii) It does not distinguish changes that result from increasing the area and atoms (H vs F) exposed on the surface of the R, from changes

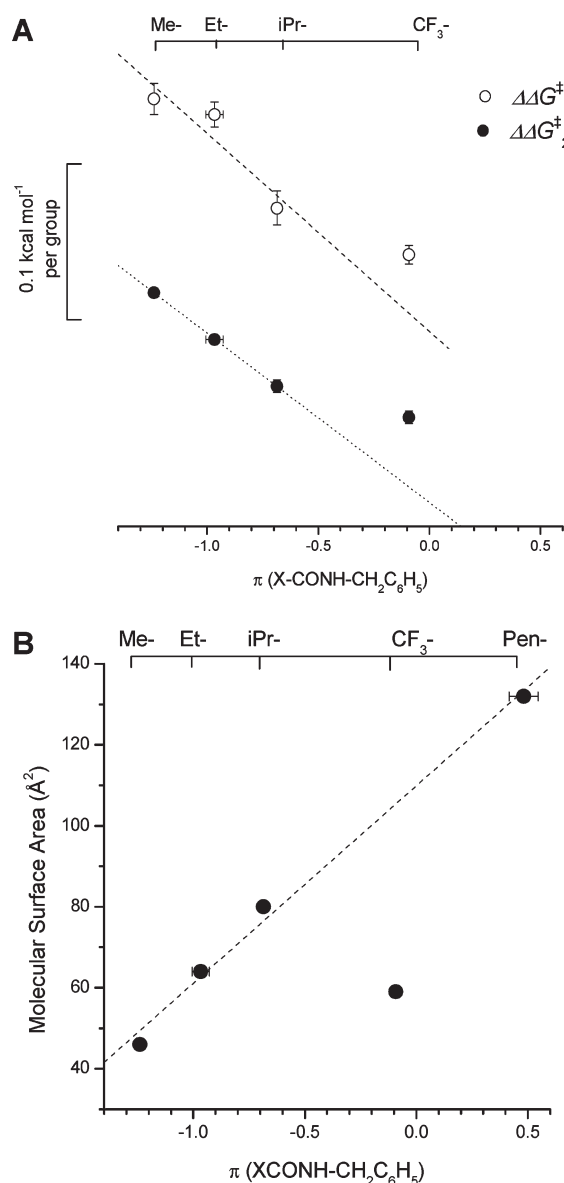


Figure 7. Influence of CF₃CONH[−] and R_HCONH[−] on the denaturation of BCA and on the water–octanol partitioning of X–CONH–CH₂C₆H₅. (A) Values of $\Delta\Delta G_1^\ddagger$ and $\Delta\Delta G_2^\ddagger$, obtained in the analysis of Figure 5, plotted against π for CF₃CONH–CH₂C₆H₅ and R_HCONH–CH₂C₆H₅. The plot uses a floating y-axis in order to show points for $\Delta\Delta G_1^\ddagger$ and $\Delta\Delta G_2^\ddagger$ on the same scale (values for $\Delta\Delta G_1^\ddagger$ decrease from +0.31 to +0.21 kcal mol^{−1} per group; values for $\Delta\Delta G_2^\ddagger$ decrease from 0.00 to −0.08 kcal mol^{−1} per group). Vertical error bars show standard errors in the fitting parameters determined in Figure 5, and the horizontal error bars show the minimum and maximum values of π from three measurements. Dashed and dotted lines were obtained by fitting to the points for Me–, Et–, and iPr–, but not CF₃–. (B) Relationship between values of molecular surface area and π for of CF₃–, R_H–, and CH₃(CH₂)₄CONH– groups.

in the amide group of RCONH[−], or from differences in polarizability between H and F. In the discussion that follows, we use the word “hydrophobicity” to mean the *effective hydrophobicity of the RCONH– group*, not of the R group alone.

CF₃CONH– Groups Are Slightly More Hydrophobic than R_HCONH– Groups of Similar Surface Area. The CF₃CONH– group has a larger wetted surface area than the CH₃CONH– group;

we thus expected the CF₃CONH– group to be more hydrophobic than the CH₃CONH– group, even if the intrinsic hydrophobicity per unit surface area were the same. Using the rates of denaturation of acylated derivatives of BCA by SDS, affected in part by the hydrophobic interactions of SDS with the acyl groups at the surface of proteins (for $n \leq 7$), we infer that CF₃CONH– are more hydrophobic (by a factor <2) than CH₃CH₂CONH– and (CH₃)₂CHCONH–, hydrocarbon acyl groups of similar surface area.

The “Hydrophobicity” of CF₃CONH– Groups Is Not Determined by Nonpolar Surface Area Alone. Our understanding of why BCA–[CF₃CONH–]_{*n*} denatures more rapidly than BCA–[R_HCONH–]_{*n*} in solutions of SDS remains incomplete. We can however conclude that the influence of CF₃– groups, in the context of primary amides (CF₃CONH–), is very similar to, but still distinguishable from, that of R_H– groups (on an area-corrected basis) by some factor other than nonpolar surface area. We suspect that the CF₃– group influences the polarity and interactions of the –CONH– group to which it is connected by inductive (or some other) effects and thus contributes to the overall “hydrophobicity” of the CF₃CONH– group. That is, the interactions of CX₃– and of CX₃CONH– (X = H, F) respond slightly differently upon exchange of H by F, even after correction for area.

The hypothesis that the inductive effect of –CF₂– and CF₃– groups can influence noncovalent interactions and molecular recognition of –CONH– is also supported by the analysis of the association of fluorocarbon-substituted benzenesulfonamide inhibitors with BCA.⁵⁷ Inhibitors containing F(CF₂)_{*n*}CH₂–CONH– “tails” (–CH₂– spacer screening the amide from fluorocarbon) showed affinities for BCA that were within 0.4 kcal mol^{−1} of inhibitors with H(CH₂)_{*n*}CH₂–CONH– with similar surface area. Inhibitors containing the linkage F(CF₂)_{*n*}–CONH– however showed greater affinity for BCA than expected on the basis of surface area alone (by ~1 kcal mol^{−1}). This result suggested that in the absence of a –CH₂– spacer, F(CF₂)_{*n*}– groups may influence the interaction between –CONH– groups and the active site. The affinity of inhibitors without an H-bond donor—inhibitors with F(CF₂)_{*n*}–CONCH₃– and H(CH₂)_{*n*}–CONCH₃– tails—were indistinguishable upon correction for differences in surface area. This series of results implicated differences in H-bonding by N–H groups as the underlying difference between the free energy of association of fluorocarbon and hydrocarbon acyl groups having similar molecular surface area.

The small differences (<0.06 kcal mol^{−1} per group) observed in this paper between derivatives of BCA with CF₃CONH– and R_HCONH– groups with similar surface area (R_H = CH₃CH₂–, (CH₃)₂CH–) may originate in differences in N–H acidity, but they may also originate from several other consequences of the inductive effect of CF₃–: basicity of the –CONH– group, dipolar interactions involving the amide, or polarizability of the π electrons of the amide. We could not establish the relative importance of these effects. The system is complex, and the mechanism of denaturation of BCA is not fully determined.

Water–octanol partitioning of model compounds provided a more straightforward way to measure “hydrophobicity”, one free of the complexity of interactions involved in the denaturation of proteins by SDS (but also one that may have limited relevance to modeling the effects of CF₃CONH– and R_HCONH– in proteins). Water–octanol partitioning data supported the hypothesis that the interactions of –CONH– contribute to the hydrophobicity of CF₃CONH–. Partition coefficients showed that the hydrophobicity of CF₃– (in relation to that of R_H– groups) is sensitive to the neighboring functional group. For example, the difference in π between

$\text{CF}_3\text{-X}$ and $\text{CH}_3\text{CH}_2\text{-X}$ is ~ 0.1 , when $\text{X} = \text{C}_6\text{H}_5$, but it is ~ 0.9 when $\text{X} = \text{-CONH-CH}_2\text{C}_6\text{H}_5$. These results suggest that the inductive effect of $\text{CF}_3\text{-}$ on $\text{CF}_3\text{CONH-}$ leads to a compound that is more hydrophobic than expected from surface area of the $\text{CF}_3\text{-}$ group alone.

$\text{CF}_3\text{CONH-}$ Groups Positioned at the Surface of Derivatives of BCA Destabilize Proteins toward Denaturation in Solutions of SDS. In most previously reported studies examining the substitution of F- or $\text{CF}_3\text{-}$ in proteins, the fluorocarbon groups are positioned within the hydrophobic interior of folded proteins and contribute to increased thermostability or resistance toward chemical denaturation. In contrast, the denaturation of $\text{BCA-[CF}_3\text{CONH-]}_n$ and $\text{BCA-[R}_\text{H}\text{CONH-]}_n$ in solutions of SDS suggests that fluorocarbon groups positioned at the surface of proteins decrease the stability of folded proteins. The analytical model developed for the kinetics of denaturation suggested that $\text{CF}_3\text{CONH-}$ groups (and $\text{R}_\text{H}\text{CONH-}$ groups) destabilize folded proteins by increasing the affinity of proteins for SDS. Chemical modification of surfaces of proteins with fluorocarbon groups may be useful for exploiting hydrophobic interactions to direct protein-protein interactions or to direct proteins to hydrophobic environments (examples include lipid membranes or the surfaces of devices used for biotechnology and analysis, such as fluorocarbon coated-tube assays⁵⁸).

■ ASSOCIATED CONTENT

S Supporting Information. Additional information as noted in the text, as well as information about experimental procedures and sources of chemicals. This material is available free of charge via the Internet at <http://pubs.acs.org>.

■ AUTHOR INFORMATION

Corresponding Author

*E-mail: gwhitesides@gmwgroup.harvard.edu.

■ ACKNOWLEDGMENT

This research was funded by NIH Award GM051559. We thank Dr. Demetri Moustakas for helpful discussions and computation of molecular surface areas.

■ REFERENCES

- (1) Gudiksen, K. L.; Gitlin, I.; Moustakas, D. T.; Whitesides, G. M. *Biophys. J.* **2006**, *91*, 298–310.
- (2) Jones, M. N. *Chem. Soc. Rev.* **1992**, *21*, 127–136.
- (3) Schneider, G. F.; Shaw, B. F.; Lee, A.; Carillho, E.; Whitesides, G. M. *J. Am. Chem. Soc.* **2008**, *130*, 17384–17393.
- (4) Turro, N. J.; Lei, X. G.; Ananthapadmanabhan, K. P.; Aronson, M. *Langmuir* **1995**, *11*, 2525–2533.
- (5) Reynolds, J. A.; Tanford, C. *Proc. Natl. Acad. Sci. U.S.A.* **1970**, *66*, 1002–1008.
- (6) Purser, S.; Moore, P. R.; Swallow, S.; Gouverneur, V. *Chem. Soc. Rev.* **2008**, *37*, 320–330.
- (7) Muller, K.; Faeh, C.; Diederich, F. *Science* **2007**, *317*, 1881–1886.
- (8) Bohm, H. J.; Banner, D.; Bendels, S.; Kansy, M.; Kuhn, B.; Muller, K.; Obst-Sander, U.; Stahl, M. *ChemBioChem* **2004**, *5*, 637–643.
- (9) Ojima, I. *ChemBiochem* **2004**, *5*, 628–635.
- (10) Stump, B.; Eberle, C.; Schweizer, W. B.; Kaiser, M.; Brun, R.; Krauth-Siegel, R. L.; Lentz, D.; Diederich, F. *ChemBioChem* **2009**, *10*, 79–83.
- (11) Sigal, G. B.; Mrksich, M.; Whitesides, G. M. *J. Am. Chem. Soc.* **1998**, *120*, 3464–3473.
- (12) Smart, B. E. *J. Fluorine Chem.* **2001**, *109*, 3–11.
- (13) Biffinger, J. C.; Kim, H. W.; DiMagno, S. G. *ChemBioChem* **2004**, *5*, 622–627.
- (14) Hagmann, W. K. *J. Med. Chem.* **2008**, *51*, 4359–4369.
- (15) Salwiczek, M.; Koks, B. *ChemBioChem* **2009**, *10*, 2867–2870.
- (16) Yoder, N. C.; Kumar, K. *Chem. Soc. Rev.* **2002**, *31*, 335–341.
- (17) Jackel, C.; Koks, B. *Eur. J. Org. Chem.* **2005**, 4483–4490.
- (18) Bilgic, B.; Kumar, K. *Proc. Natl. Acad. Sci. U.S.A.* **2004**, *101*, 15324–15329.
- (19) Vagt, T.; Nyakatura, E.; Salwiczek, M.; Jackel, C.; Koks, B. *Org. Biomol. Chem.* **2010**, *8*, 1382–1386.
- (20) Chiu, H. P.; Suzuki, Y.; Gullickson, D.; Ahmad, R.; Kokona, B.; Fairman, R.; Cheng, R. P. *J. Am. Chem. Soc.* **2006**, *128*, 15556–15557.
- (21) Woll, M. G.; Hadley, E. B.; Mecozzi, S.; Gellman, S. H. *J. Am. Chem. Soc.* **2006**, *128*, 15932–15933.
- (22) Horng, J. C.; Raleigh, D. P. *J. Am. Chem. Soc.* **2003**, *125*, 9286–9287.
- (23) Son, S.; Tanrikulu, I. C.; Tirrell, D. A. *ChemBioChem* **2006**, *7*, 1251–1257.
- (24) Jackel, C.; Seufert, W.; Thust, S.; Koks, B. *ChemBioChem* **2004**, *5*, 717–720.
- (25) Montclare, J. K.; Son, S.; Clark, G. A.; Kumar, K.; Tirrell, D. A. *ChemBioChem* **2009**, *10*, 84–86.
- (26) Jackel, C.; Salwiczek, M.; Koks, B. *Angew. Chem., Int. Ed.* **2006**, *45*, 4198–4203.
- (27) Dunitz, J. D. *ChemBioChem* **2004**, *5*, 614–621.
- (28) $\pi = \log(P_\text{R}/P_\text{H})$, where P_R and P_H are partition coefficients for compounds with the substituents R- or H- .
- (29) Fujita, T.; Hansch, C.; Iwasa, J. *J. Am. Chem. Soc.* **1964**, *86*, 5175–5185.
- (30) Abraham, M. H.; Chadha, H. S.; Dixon, J. P.; Leo, A. J. *J. Phys. Org. Chem.* **1994**, *7*, 712–716.
- (31) Abraham, M. H.; Dearden, J. C.; Bresnen, G. M. *J. Phys. Org. Chem.* **2006**, *19*, 242–248.
- (32) The partitioning of $\text{CF}_3\text{CO}_2\text{H}$ and $\text{CF}_3\text{COCH}_2\text{R}$ indicates that they are less hydrophobic than expected; the inductive effect of $\text{CF}_3\text{-}$ is believed to be responsible, by increasing the strength of hydrogen bonds or by favoring the formation of hydrates (in the case of $\text{CF}_3\text{COCH}_2\text{R}$). The inductive effect of $\text{CF}_3\text{-}$ on acid-base properties and chemical reactivity are well-known; substituting $\text{CH}_3\text{-}$ groups with $\text{CF}_3\text{-}$ groups can increase Bronsted acidity by as much 4–5 pK_a units (examples given in Table 1).
- (33) Values of MSA were calculated using the software program MOE, developed by the Chemical Computing Group (Montreal, Canada).
- (34) Values of $\log P$ for the compounds $\text{CF}_3\text{CONHCH}_2\text{-C}_6\text{H}_5$ and $\text{R}_\text{H}\text{CONHCH}_2\text{-C}_6\text{H}_5$ were obtained in water-octanol partitioning experiments for this paper.
- (35) Hildebrand, J. H. *Regular and Related Solutions; The Solubility of Gases, Liquids, And Solids*; Van Nostrand Reinhold Co.: New York, 1970.
- (36) Abraham, M. H.; Platts, J. A. *J. Org. Chem.* **2001**, *66*, 3484–3491.
- (37) Schwobel, J.; Ebert, R. U.; Kuhne, R.; Schuurmann, G. *J. Phys. Chem. A* **2009**, *113*, 10104–10112.
- (38) Gitlin, I.; Carbeck, J. D.; Whitesides, G. M. *Angew. Chem., Int. Ed.* **2006**, *45*, 3022–3060.
- (39) Carbeck, J. D.; Colton, I. J.; Anderson, J. R.; Deutch, J. M.; Whitesides, G. M. *J. Am. Chem. Soc.* **1999**, *121*, 10671–10679.
- (40) ΔZ is less than a full unit of charge due to charge regulation and is close to -0.9 for the first few acylations at $\text{pH} = 8.4$. One plausible reason for a value of ΔZ that is less than a full unit of charge is a small change in the local pH or a shift in pK_a for some ionizable residues of the protein.
- (41) Gudiksen, K. L.; Gitlin, I.; Yang, J.; Urbach, A. R.; Moustakas, D. T.; Whitesides, G. M. *J. Am. Chem. Soc.* **2005**, *127*, 4707–4714.
- (42) Gitlin, I.; Gudiksen, K. L.; Whitesides, G. M. *ChemBioChem* **2006**, *7*, 1241–1250.

(43) Gitlin, I.; Gudiksen, K. L.; Whitesides, G. M. *J. Phys. Chem. B* **2006**, *110*, 2372–2377.

(44) Anderson, J. R.; Cherniavskaya, O.; Gitlin, I.; Engel, G. S.; Yuditky, L.; Whitesides, G. M. *Anal. Chem.* **2002**, *74*, 1870–1878.

(45) Schwartz, B.; Druekhammer, D. G.; Usher, K. C.; Remington, S. J. *Biochemistry* **1995**, *34*, 15459–15466.

(46) The inductive effect probably results in stronger N–H donors and weaker C=O acceptors in CF₃CONH– groups (compared to those of R_HCONH– groups). Details about the effect of CF₃– groups on the acidity and hydrogen bonding of amides are not available in the literature. Estimates for the pK_a of acetamide span the range ~15–17 (aqueous solution, 22 °C). Two reports analyzing the acidity of trifluoroacetamide disagree on the value of pK_a. The more recent study by Comuzzi (ref 41) was skeptical of a previously reported value of 10.4 for the pK_a of trifluoroacetamide (ref 42) and suggested a pK_a > 14 but could not analyze trifluoroacetamide in solutions with [OH[–]] > 1 M due to its rapid hydrolysis.

(47) Bagno, A.; Comuzzi, C. *Eur. J. Org. Chem.* **1999**, 287–295.

(48) Kashik, T. V.; Rassolova, G. V.; Ponomareva, S. M.; Medvedeva, E. N.; Yushmanova, T. I.; Lopyrev, V. A. *B. Acad. Sci. USSR Ch. Sci.* **1982**, *31*, 1965–1968.

(49) Structures of BCA and BCA–[CH₃CONH–]₁₈ solved by X-ray crystallography indicate that the conversion of Lys-ε-NH₃⁺ to CH₃CONH– results in a rearrangement of hydrogen bonds involving the side chain of six of 18 Lys residues (unpublished observations). Acetylation of Lys111, Lys125, Lys166, Lys211, and Lys223 leads to the creation of a hydrogen bond between the N–H donor of Lys-ε-CH₃CONH– and neighboring groups at the surface of BCA–[CH₃CONH–]₁₈; the structure solved for BCA does not show hydrogen bonding by the ε-NH₃⁺ groups of these lysine residues.

(50) Chan, C. K.; Hu, Y.; Takahashi, S.; Rousseau, D. L.; Eaton, W. A.; Hofrichter, J. *Proc. Natl. Acad. Sci. U.S.A.* **1997**, *94*, 1779–1784.

(51) Comuzzi et al. proposed that the pK_a of trifluoroacetamide > 14. Assuming values of pK_a near or greater than 14, CF₃CONH– groups should not be ionized to an appreciable extent (fractions of ~10^{–6}) in Tris–Gly buffer.

(52) Mass transport across the dialysis membranes we used (10 kDa cutoff) is rapid for low molecular weight compounds. Observation of probe compounds (e.g., DMF by UV-absorbance) reveals a ~20-fold decrease in concentration within ~5 min when samples are dialyzed against buffer solutions.

(53) Unfolded and aggregated BCA, generated by heating to temperatures beyond the T_m (65 °C, ref 49), has a value of μ (6–12 cm² kV^{–1} min^{–1}) higher than that of native BCA (4 cm² kV^{–1} min^{–1}).

(54) Krishnamurthy, V. M.; Kaufman, G. K.; Urbach, A. R.; Gitlin, I.; Gudiksen, K. L.; Weibel, D. B.; Whitesides, G. M. *Chem. Rev.* **2008**, *108*, 946–1051.

(55) Westerhuis, W. H. J.; Sturgis, J. N.; Niederman, R. A. *Anal. Biochem.* **2000**, *284*, 143–152.

(56) Hilser, V. J.; Freire, E. *Anal. Biochem.* **1995**, *224*, 465–485.

(57) Gao, J. M.; Qiao, S.; Whitesides, G. M. *J. Med. Chem.* **1995**, *38*, 2292–2301.

(58) Kobos, R. K.; Eveleigh, J. W.; Arentzen, R. *Trends Biotechnol.* **1989**, *7*, 101–105.